

# PROBE COMPENSATION CHARACTERIZATION IN CYLINDRICAL NEAR-FIELD SCANNING'

Ziad A. Hussein  
Jet Propulsion Laboratory  
California Institute of Technology  
Pasadena, CA 91109

Yahya Rahmat-Samii  
University of California Los Angeles  
Department of Electrical Engineering  
Los Angeles, CA 90024-1594

1. INTRODUCTION Probe pattern compensation is necessary in near-field scanning geometry, where there is a great need to accurately know far-field pattern at wide angular range. For example, in a recent study for the NASA scatterometer slotted waveguide radar antenna, there is need for an accurate assessment of performance at wide angles. This paper presents a useful computer simulation methodology to properly characterize the role of probe compensation in cylindrical near-field scanning. The methodology is applied to a linear test array antenna and has been applied to other antenna configurations.

2. ANALYSIS Consider an idealized circular aperture probe that is modeled by its equivalent tangential electric currents,  $J_s$ , in the  $x_p=0$  plane of the probe coordinate system shown in Figure 1. The currents on the circular aperture plane can be written as

$$\begin{aligned} J_s &= \hat{x}_p \times H_p \\ M_s &= -\hat{x}_p \times E_p = 0 \end{aligned} \quad (1)$$

The interaction between the probe equivalent aperture currents and the test antenna fields,  $(E_a, H_a)$ , can be obtained with the application of reciprocity theorem to yield to the probe vector output pickup (neglecting multiple scattering)

$$P^{(1,2)} = \int_{S_p} (M_s \cdot H_a - J_s \cdot E_a) ds = - \int_{S_p} J_s \cdot E_a ds \quad (2)$$

In equation (2), superscripts (1,2) designate two orientations of the probe necessary to construct the far-field pattern of the test antenna. Specifically,  $P^1$  and  $P^2$  correspond to the probe response for the electric current,  $J_s$ , oriented in the  $z_p$  and  $-y_p$  direction respectively. Assuming a uniform current across the probe, the integral in equation (2) is then approximated by

---

<sup>1</sup>The research work described in this paper was carried out by Jet Propulsion Laboratory, California Institute of Technology, under contract with National Aeronautics and Space Administration.

$$P^1 \approx \int_{S_p} E_z(\rho, \phi, z) \rho_p d\phi_p d\rho_p \quad P^2 \approx \int_{S_p} E_\phi(\rho, \phi, z) \rho_p d\phi_p d\rho_p \quad (3)$$

where  $(\rho_p, \phi_p)$  defines the polar coordinate in the aperture of the probe,  $S_p$ , and  $E_z, E_\phi$  are the fields in cylindrical coordinate system of the test antenna computed on the probe aperture, '1 he use of an idealized circular aperture probe, with different radius, permits us to derive a closed form expression for its far-field radiation pattern. For a uniform magnetic field,  $H_{y_p}$ , in the aperture of the probe oriented in the  $y_p$  direction, the probe pattern is given by

$$E_{\theta p}^1 = \sin\theta_p \frac{J_1(u)}{u} \hat{\theta}_p \quad E_{\phi p}^1 = 0 \hat{\phi}_p \quad (4)$$

and for a  $90^\circ$  rotation of it yields

$$E_{\theta p}^2 = \cos\theta_p \sin\phi_p \frac{J_1(u)}{u} \hat{\theta}_p \quad E_{\phi p}^2 = \cos\phi_p \frac{J_1(u)}{u} \hat{\phi}_p \quad (5)$$

where  $u = ka \sin(\alpha)$ ,  $\cos(\alpha) = \sin(\theta_p) \cos(\phi_p)$ ,  $a$  is the probe radius,  $k$  is the wavenumber  $2\pi/\lambda$  and  $J_1(u)$  is the Bessel function of the first kind. To perform probe pattern compensation, one needs the cylindrical wave expansion of the probe fields from the following expressions (assuming no fields in the back of the probe)

$$a_m^2(k \cos\theta_p) = \frac{1}{j^m \sin\theta_p} \int_{-\pi/2}^{\pi/2} E_{\phi p}^2(\theta_p, \phi_p) \tilde{\sigma}^{jm} \phi_p d\phi_p \quad (6)$$

$$b_m^2(k \cos\theta_p) = \frac{1}{j^{m+1} \sin\theta_p} \int_{-\pi/2}^{\pi/2} E_{\theta p}^2(\theta_p, \phi_p) \tilde{\sigma}^{-jm} \phi_p d\phi_p$$

where  $m < ka$ . Similarly, one could obtain the probe coefficients,  $a_m^1$  and  $b_m^1$ , for the other field components  $E_{\theta p}^1$  and  $E_{\phi p}^1$ . These results, together with the probe vector output pickup (equations 3-6 are numerically evaluated) allows us to perform computer simulated synthetic measurements. The test antenna fields,  $E$  and  $E_\phi$ , are then constructed in terms of the probe vector output pickup and probe antenna coefficients derived from application of reciprocity theorem [1-2]

$$E_\phi^t(\theta, \phi) = \sin\theta \sum_{|n| < kr} j^n a_n(k \cos\theta) e^{jn\phi} \hat{\theta} \quad (7)$$

$$E_\theta^t(\theta, \phi) = \sin\theta \sum_{|n| < kr} j^{n+1} b_n(k \cos\theta) e^{jn\phi} \hat{\phi}$$

where  $r$  is the smallest radius enclosing the test antenna and  $a_n, b_n$  are given by

$$a_n(k \cos \theta) = - \frac{T_n^1(k \cos \theta) \alpha_m^2(k \cos \theta) - T_n^2(k \cos \theta) \alpha_m^1(k \cos \theta)}{\sin^2 \theta \Delta_n(k \cos \theta)} \quad (8)$$

$$b_n(k \cos \theta) = - \frac{T_n^2(k \cos \theta) \gamma_m^1(k \cos \theta) - T_n^1(k \cos \theta) \gamma_m^2(k \cos \theta)}{\sin^2 \theta \Delta_n(k \cos \theta)}$$

$$T_n^{(1,2)}(k \cos \theta) = \int_{-\infty}^{\infty} \int_{-\pi}^{\pi} P^{(1,2)} \tilde{e}^{jn\phi} \tilde{e}^{jk \cos \theta z} d\phi dz \quad (9)$$

$$\Delta_n(k \cos \theta) = \gamma_m^1(k \cos \theta) \alpha_m^2(k \cos \theta) - \gamma_m^2(k \cos \theta) \alpha_m^1(k \cos \theta)$$

$$\alpha_m^{(1,2)}(k \cos \theta) = \sum_{|m| < k a} b_m^{(1,2)}(k \cos \theta_p) H_{n+m}^2(k r_0 \sin \theta) \quad (10)$$

$$\gamma_m^{(1,2)}(k \cos \theta) = \sum_{|m| < k a} a_m^{(1,2)}(k \cos \theta_p) H_{n+m}^2(k r_0 \sin \theta)$$

where  $H_{n+m}^2$  is the hankel function of the second kind and  $r_0$  is the sampling cylinder radius. In the limit as the probe radius becomes very small, the probe output pickup, equation (2), is the direct response of the near-field at a point, that is the response of infinitesimal hertzian dipole,  $P^1 = E_z$  and  $P^2 = E_\phi$ , and no probe compensation is needed.

**3. DISCUSSION & RESULTS** Useful results are generated to compare the far-field pattern (copolar and crosspolar) of the test antenna constructed from the knowledge of the simulated near-field with and without probe pattern compensation and the exact results. Representative cases are shown in Figure 2 for a seven element linear array. It has been found that a probe with a low directivity, 5.5dB, aperture radius of  $0.3\lambda$ , requires little probe correction at wide angular range. A probe with an aperture radius of  $0.5\lambda$ , and  $1\lambda$ , higher directivity, needs a little if any probe correction near the antenna main beam, and requires significant probe correction at wide angle in the constructed patterns. Similar observations were made for a highly directive test antennas. Also we note that for a highly directive probe, e.g.,  $a=1\lambda$ , probe compensation may not be possible at the probe null since  $\Delta_n$  goes to zero and this is shown in Figure 2c.

#### 4. REFERENCES

- [1] Yaghjian, A.D "Near-Field Antenna Measurement On A Cylindrical Surface: A Source Scattering-Matrix Formulation", NBS Tech. Note 696, July 1977.
- [2] Leach W. M. Jr. and Paris D.T. " Probe Compensated Near-Field Measurements on a Cylinder" IEEE Trans, AP., vol. AP-21 No.4, pp 435-445, July 1973.

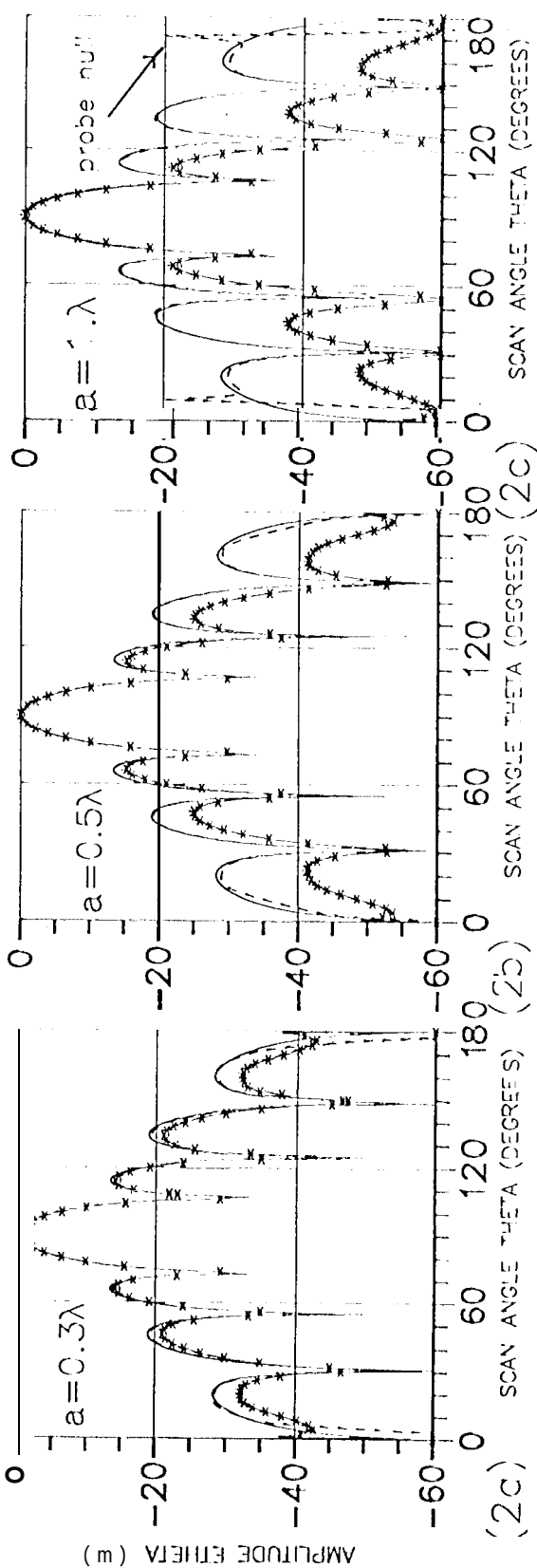
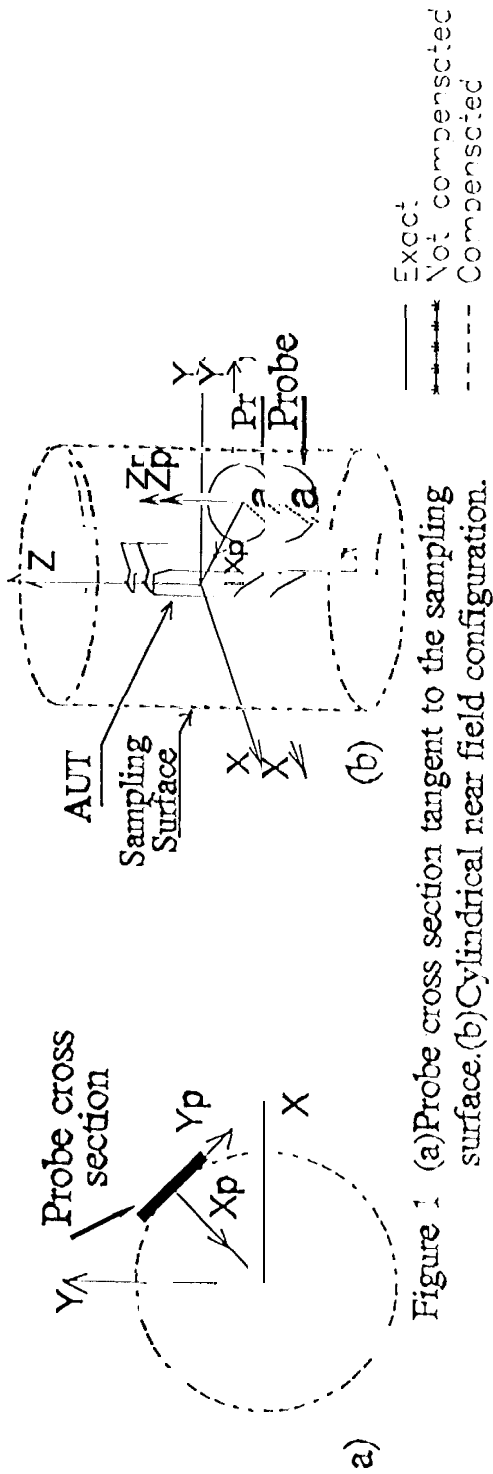


Figure 2. For-field pattern of a seven-element array constructed from simulated near-field with and without probe pattern compensation. (2a) corresponds to a probe with directivity 5.5dB, (2b) 9.94 dB and (2c) 15.96 dB.